

# Clinical Cancer Research



## Value of Magnetic Resonance Spectroscopy Imaging and Dynamic Contrast-Enhanced Imaging for Detecting Prostate Cancer Foci in Men With Prior Negative Biopsy

Alessandro Sciarra, Valeria Panebianco, Mauro Ciccariello, et al.

*Clin Cancer Res* 2010;16:1875-1883. Published OnlineFirst March 2, 2010.

**Updated Version** Access the most recent version of this article at:  
doi:[10.1158/1078-0432.CCR-09-2195](https://doi.org/10.1158/1078-0432.CCR-09-2195)

**Cited Articles** This article cites 27 articles, 5 of which you can access for free at:  
<http://clincancerres.aacrjournals.org/content/16/6/1875.full.html#ref-list-1>

**Citing Articles** This article has been cited by 3 HighWire-hosted articles. Access the articles at:  
<http://clincancerres.aacrjournals.org/content/16/6/1875.full.html#related-urls>

**E-mail alerts** [Sign up to receive free email-alerts](#) related to this article or journal.

**Reprints and Subscriptions** To order reprints of this article or to subscribe to the journal, contact the AACR Publications Department at [pubs@aacr.org](mailto:pubs@aacr.org).

**Permissions** To request permission to re-use all or part of this article, contact the AACR Publications Department at [permissions@aacr.org](mailto:permissions@aacr.org).

**Imaging, Diagnosis, Prognosis****Value of Magnetic Resonance Spectroscopy Imaging and Dynamic Contrast-Enhanced Imaging for Detecting Prostate Cancer Foci in Men With Prior Negative Biopsy**

Alessandro Sciarra<sup>1</sup>, Valeria Panebianco<sup>2</sup>, Mauro Ciccariello<sup>2</sup>, Stefano Salciccia<sup>1</sup>, Susanna Cattarino<sup>3</sup>, Danilo Lisi<sup>2</sup>, Alessandro Gentilucci<sup>1</sup>, Andrea Alfaroni<sup>1</sup>, Silvia Bernardo<sup>2</sup>, Roberto Passariello<sup>2</sup>, and Vincenzo Gentile<sup>1</sup>

**Abstract**

**Purpose:** This study aimed to prospectively analyze the role of magnetic resonance spectroscopy imaging (MRSI) and dynamic-contrast enhancement magnetic resonance (DCEMR) in the detection of prostate tumor foci in patients with persistently elevated prostate-specific antigen levels (in the range of  $\geq 4$  ng/mL to  $<10$  ng/mL) and prior negative random trans-rectal ultrasound (TRUS)-guided biopsy.

**Experimental Design:** This was a prospective randomized single-center study. One hundred and eighty eligible cases were included in the study. Patients in group A were submitted to a second random prostate biopsy, whereas patients in group B were submitted to a <sup>1</sup>H-MRSI-DCEMR examination and samples targeted on suspicious areas were associated to the random biopsy.

**Results:** At the second biopsy, a prostate adenocarcinoma histologic diagnosis was found in 22 of 90 cases (24.4%) in group A and in 41 of 90 cases (45.5%) in group B ( $P = 0.01$ ). On a patient-by-patient basis, MRSI had 92.3% sensitivity, 88.2% specificity, 85.7% positive predictive value (PPV), 93.7% negative predictive value (NPV), and 90% accuracy; DCEMR had 84.6% sensitivity, 82.3% specificity, 78.5% PPV, 87.5% NPV, and 83.3% accuracy; and the association MRSI plus DCEMR had 92.6% sensitivity, 88.8% specificity, 88.7% PPV, 92.7% NPV, and 90.7% accuracy, for predicting prostate cancer detection.

**Conclusions:** The combination of MRSI and DCEMR showed the potential to guide biopsy to cancer foci in patients with previously negative TRUS biopsy. To avoid a potential bias, represented from having taken more samples in group B (mean of cores, 12.17) than in group A (10 cores), in the future a MRSI/DCEMR directed biopsy could be prospectively compared with a saturation biopsy procedure. *Clin Cancer Res*; 16(6); 1875–83. ©2010 AACR.

At present, suspicion of prostate adenocarcinoma is mainly based on three tests: digital rectal examination, prostate-specific antigen (PSA), and trans-rectal ultrasound (TRUS), and is confirmed by TRUS-guided biopsies. The latter is recognized by urologists as the first choice in the diagnosis of prostate pathologies (1). All three modern imaging modalities, namely, computer tomography, ultrasonography, and magnetic resonance (MR), have been considered to have limitations in the diagnosis of prostate adenocarcinoma. Recently some studies (2–5) revealed the high diagnostic accuracy of

combined proton <sup>1</sup>H-magnetic resonance spectroscopic imaging (<sup>1</sup>H-MRSI) and dynamic contrast-enhanced imaging magnetic resonance (DCEMR) in the management of prostate cancer. The advantage of MRSI is that the spectroscopic analysis provides metabolic information regarding prostatic tissue by displaying the relative concentrations of chemical compounds within contiguous small volumes of interest (voxels). In the prostate the substances analyzed by MRSI are citrate, creatine, and choline. For practical purposes, prostate adenocarcinoma can be distinguished from healthy peripheral zone tissue on the basis of the (choline + creatine)/citrate ratio (5–7). Normal peripheral zone tissue is characterized by voxels with a (choline + creatine)/citrate ratio of  $<0.8$ ; suspicious of cancer is defined as a voxel with (choline + creatine)/citrate ratio  $>0.8$  (8).

DCEMR consists in the acquisition of sequential images using T1-weighted sequences during the passage of a contrast agent (gadopentetate dimeglumine) within the prostatic tissue. The technique is based on the assessment of

**Authors' Affiliations:** Departments of <sup>1</sup>Urology and <sup>2</sup>Radiology, University Sapienza, and <sup>3</sup>Department of Urology, University of Rome, Rome, Italy

**Corresponding Author:** Alessandro Sciarra, Department of Urology, University Sapienza, Viale Policlinico 155, 00161 Rome, Italy. Phone: 06-49974204; Fax: 06-49974280; E-mail: sciarra.md@libero.it.

doi: 10.1158/1078-0432.CCR-09-2195

©2010 American Association for Cancer Research.

### Translational Relevance

Men with persistently elevated serum prostate-specific antigen (PSA) levels after a negative first random trans-rectal ultrasound (TRUS)-guided prostate biopsy represent a great diagnostic challenge for urologists.

In this current prospective, randomized study we analyzed the role of magnetic resonance spectroscopy imaging (MRSI) and dynamic-contrast enhancement magnetic resonance (DCEMR) in the detection of prostate tumor foci in patients with persistently elevated PSA levels and prior negative random TRUS-guided biopsy. The present is the largest randomized prospective study in the literature showing that, in patients with a prior negative prostate biopsy and persistent elevated PSA levels, a combination of a standard 10-core biopsy scheme with an oversampling strategy in sites targeted by combined MRSI/DCEMR indications, resulted in significantly higher cancer detection rates.

This should represent a reasonable approach in a group of patients who often have tremendous psychological stresses due to the uncertain diagnosis obtained with random repeated biopsies in the face of persistently abnormal PSA.

tumor neoangiogenesis, which is an integral feature of tumors (9). In contrast to angiogenesis in normal tissues where this process is a well-organized event, in tumors angiogenesis is chaotic. Furthermore, because the amount of interstitial space is greater in cancerous tissue than in normal tissue, there is a larger gap of contrast material concentration between the plasma and the interstitial tissue. This characteristic environment makes the enhancement pattern of cancerous tissue different from that of normal tissue (9).

Random TRUS-guided biopsy is now the preferred method for histologic diagnosis of prostate adenocarcinoma. Some studies emphasized that random biopsies miss out 30% of cancers (6). Men with persistently elevated serum PSA levels after a negative first random TRUS-guided prostate biopsy represent a great diagnostic challenge for urologists (10). The fact that additional rounds of conventional random biopsies do not improve the cancer detection rate in this group of patients shows the high false-negative rates of the current random biopsy technique (10–13). On the basis of these outcomes there is a need for a more sensitive and accurate imaging modality to direct biopsy and to detect prostate cancer. The aim of the present randomized study was to prospectively analyze the role of MRSI and DCEMR in the detection of prostate tumor foci in patients with persistently elevated PSA levels (in the range of  $\geq 4$  ng/mL and  $< 10$  ng/mL) and prior negative random TRUS-guided biopsy. As in previous studies (14, 15) we limited our analysis to this range of PSA because the greatest clinical problem occurs

in men with a PSA level between 4 ng/mL and 10 ng/mL, in which it is more important to reduce unnecessary biopsies and to improve biopsy targeting.

### Materials and Methods

**Study design and population.** This was a prospective randomized single-center study on patients with prior negative random TRUS-guided prostate biopsy and persistent elevated PSA levels.

This study was conducted after approval of the protocol from our institutional board committee and informed consent for inclusion was obtained from all patients. We recruited into the study 215 consecutive patients referred to our Urologic Clinic in a period from January 2007 to January 2009. Age of the patients ranged between 49 and 74 y (mean, 63.5 y) and all cases had a first random TRUS-guided prostate biopsy negative for prostate adenocarcinoma or high-grade prostate intraepithelial neoplasia, persistent elevated PSA levels (total PSA  $\geq 4$  ng/mL and  $< 10$  ng/mL), and negative digital rectal examination.

Exclusion criteria for the study were previous hormonal, surgical, or radiation therapies for prostate diseases, and cases in which a MR with a complete MRSI and DCEMR study was not possible.

Inclusion criteria for the study were first negative (no histologic diagnosis of prostate cancer or preneoplastic lesions) prostate biopsy, persistent total PSA  $\geq 4$  ng/mL and  $< 10$  ng/mL, and negative digital rectal examination.

All first biopsies were homogeneously done in our Department by the same physician (MC), as part of the patients' urological work-up (10-core laterally directed random TRUS-guided prostate biopsy).

One hundred and eighty eligible cases were included in the study. Patient characteristics at inclusion are described in Table 1.

After their consensus patients were therefore randomly (1:1) assigned to two groups (Fig. 1):

Group A: a second random prostate biopsy was directly done no later than 60 d from the first prostate biopsy (10 cores).

Group B: a  $^1\text{H}$ -MRSI-DCEMR examination was done (at least 30 d from the first biopsy). The second random prostate biopsy was done no later than 60 d from the first prostate biopsy and no later than 2 wk from MRI. In cases of prostate areas described by MRSI and/or DCEMR as suspicious for cancer, samples targeted on these areas were associated to the random biopsy (mean of cores, 12.17; SD, 2.296; range, 10–16).

In group A, after a second negative random biopsy, cases were offered to receive a MRSI/DCEMR, and a third random biopsy plus targeted samples, in case of prostate areas described by MRSI and/or DCEMR as suspicious for cancer, was done no later than 60 d from the second biopsy and no later than 2 wk from MRI.

**Prostatic biopsy.** As with the first negative biopsy, all prostate biopsies during the randomized trial were done

in our department by a single physician (MC) with long experience in this procedure. All TRUS and biopsies were done using an end-fire ultrasound transducer and biopsy gun with an 18-gauge needle (Esaote Technos MP with a C10-5 transducer). Prostatic volumes were assessed using the prolate ellipsoid method. As common practice in our institution (14), standard random, laterally directed 10-core (two cores from the basal portion; lateral and paramedial), two from the midgland (lateral and paramedial), and one from the apex (on each side of the gland) biopsies were done for each patient (Fig. 2A). In the cases with areas described by MRSI/DCEMR as suspicious for cancer, two additional cores were taken from each site labeled abnormal. Biopsy targeting was done in zones corresponding to those analyzed with MRSI and DCEMR, on the basis of the *x*- and *z*-coordinates derived from the T2-weighted MRI, as previous described.

Each biopsy core was labeled, processed, and examined separately by our pathologist. All histologic assessments were done blinded to MRI results. Presence, location, and Gleason grade of prostate cancer for each biopsy sample were determined in all cases.

**MRI and MRSI-DCEMR.** All examinations were done on a commercially available 1.5 T scanner (Magnetom Avanto, Siemens Medical Solutions; gradient strength, 45 mT/m; slew rate, 346 T/m/s; rise time, 400 micro/s; featuring total imaging matrix-TIM1 technology), equipped with surface phased array (Body Matrix, Siemens Medical Solutions) and endorectal coil, filled with 70 to 90 mL of air on the basis of patient tolerance (e-Coil, Medrad, combined with Endo-Interface, Siemens Medical Solutions). Morphologic imaging of the prostatic gland was done by acquiring turbo spin echo (TSE) T2-weighted sequences in the axial, sagittal, and coronal planes, with the use of optimized parameters for a better spatial resolution [repetition time (TR), 5,190 ms; echo time (TE), 95 ms; flip angle, 1,508; average, 3; field of view (FOV) read, 256 mm; FOV phase, 100; thickness, 3 mm; section gap, 0; ma-

trix, 512 \_ 512; phase resolution, 100%; band width, 130; scan time, 3.40 min).

The technique used for MR imaging, <sup>1</sup>H-MRSI, and DCEMR of the prostate has been previously described (16).

At <sup>1</sup>H-MRSI, a point-resolved spectroscopic sequence was obtained with the use of three-dimensional (3D) chemical shift imaging sequence with spectral/spatial pulses optimized for quantitative detection of choline and citrate. (FoV, 50 × 50 × 50 mm; Vol (volume of interest), 30 × 30 × 30 mm; TR, 700 ms; TE, 120 ms; flip angle, 55°; interpolation, 16; vector size, 512; TA, 11.50 min;  $\delta$  frequency, -1.80 ppm; average, 6; voxel isotropic, 0.3 cm<sup>3</sup>).

DCEMR images were acquired by using a Gradient-Echo (GRE) T1-weighted sequence during i.v. contrast agent administration (TR, 2.0 ms; TE, 1.0 ms; flip angle, 19°; average, 1; thickness, 4 mm; section gap, 0; time resolution, 12 sections/3 s; matrix, 256 × 256; scan time, 3.50 min) immediately following completion of an i.v. bolus injection of 1.0 mmol/mL of Gadobutrol (Gadovist, Bayer Shering Pharma AG). Contrast was administered with a power injector (Spectris, Medrad) at 3.0 mL/s and was followed by a 15 mL saline flush. During contrast agent administration, subtraction images were generated by an automated algorithm that uses the first 3 s of the sequence as baseline for the following measurements. We used this technique to improve regions of interest (ROI) placing, in subsequent signal intensity time (SI-T) concentration curves analysis.

The 3D volume was acquired with the same positioning angle and center as the transverse T2-weighted sequence, covering the entire prostate gland. Relative gadolinium chelate concentration curves were calculated.

**<sup>1</sup>H-MRSI and DCMRE data analysis.** MR images were analyzed in consensus by two radiologists with long experience in urogenital MRI (VP and RP). As in previous studies (17, 18), for comparison of MR with pathologic data, the peripheral zone of the prostate was divided into sextant

**Table 1.** Characteristics of the population randomized in group A and group B

Parameters	Group A	Group B	P
No. of cases	90	90	—
Total PSA (ng/mL), mean ± SD (median; range)	6.30 ± 0.91 (6.0; 4.0-9.0)	6.22 ± 1.03 (6.2; 4.0-9.3)	0.580
Prostate volume (cc), mean ± SD (median; range)	42.17 ± 7.47 (45.0; 30.0-60.0)	43.81 ± 7.55 (45.5; 30.0-63.0)	0.460
Familiarity for prostate cancer	0	0	—
Suspicious at MRSI, no. of cases (%)	—	6 (6.67)	
Suspicious at DCEMR, no. of cases (%)	—	3 (3.33)	
Suspicious at both MRSI and DCEMR, no. of cases (%)	—	36 (40.0)	
Prostate cancer at second biopsy, no. of cases (%)	22 (24.40)	44 (48.88)	0.01
Prostate cancer Gleason score <7 (3+4), no. of cases (%)	9 (40.90)	16 (39.0)	0.560
Prostate cancer Gleason score ≥7 (4+3), no. of cases (%)	13 (59.10)	25 (61.0)	0.450

NOTE: P value: Mann-Whitney test.

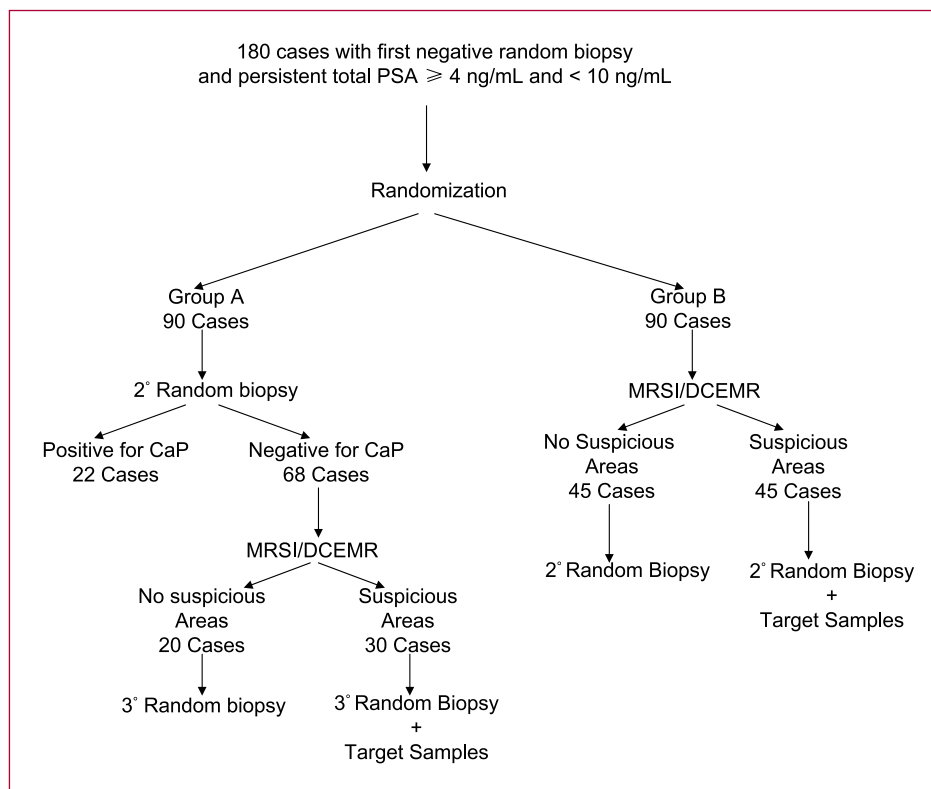


Fig. 1. Study design. CaP, prostate adenocarcinoma.

according to the following criteria: the base was defined as the upper third, which extended from the vesical margin of the prostate to the axial level with the largest transverse diameter; the mid-region was defined as the central third from the axial level to the level of the ejaculatory duct orifices at the veru montanum; the apex was defined as the remaining inferior portion of the prostate (Fig. 2B). The left and right sides of the prostate were separated by the median sagittal plane through the veru montanum. The location of MRSI voxels and DCEMR areas used for the analysis was correlated with the sextants defined by MRI. For each available voxel, absolute values (ppm) of choline, creatine, and citrate were calculated. Ratio value from choline plus creatine to citrate was obtained in all patients groups. Exams were excluded when MR spectra showed substantial lipid contamination or poor spectral signal-to-noise ratio. Voxels were classified as suspicious if the (choline + creatine)/citrate ratio was  $>0.8$  (19) and were then localized in the peripheral zone according to the described site-scheme (Fig. 2B). Voxels with elevated ratio overlapping with high intensity T1-weighted areas were not considered suspicious but were referred as artifacts from postbiopsic hemorrhage (20). Therefore, at MRSI, prostate cancer was suspected if one or more suspicious prostate voxels were identified.

The dynamic MR postprocessing procedure was done in 10 min per patient and the same radiologists reviewed

the subtracted DCE-MRI images on the basis of maximum and minimum enhancing regions. Three ROIs were drawn: on a pelvic baseline reference (pelvic muscle), on enhancing region (suspicious for lesion), and on the other side (on apparent healthy prostate tissue) as opposed to contralateral enhancing region detected. In particular, regions of CaP within the peripheral zone were identified, based on decreased signal intensity (if decrease was present) on T2-weighted MRI and higher enhancing values on subtracted images (qualitative method), according to the described site-scheme. Correspondingly, normal peripheral zone tissue was identified as having high-intermediate signal intensity on T2-weighted MRI and homogenous or no enhancing regions. When multiple enhancing regions were identified, the SI-T records of the most enhancing ROI (between ROIs placed on each region) were considered significant for subsequent analysis. Functional dynamic imaging parameters were estimated via the SI-T curves modeled with three main enhancement records: onset time of signal enhancement, time to peak, and peak enhancement (21).

**Correlation of MR findings with pathologic findings and statistical analysis.** Assessment of the spatial correspondence between MRSI and DCEMR findings and the pathologic evaluation was independently done in all cases by two investigators (VP and RP) and then revised by a third investigator (LD) who was not a reader of MR images. This

correspondence was done on the basis of the *x*- and *z*-coordinates derived from the T2-weighted MRI and on the basis of the sextant division of the peripheral zone of the prostate, as described in the previous section (MRSI and DCEMR data analysis).

Statistical data analysis was done with the statistical software MedCalc Software Demo for Windows, version 9.3. A *P* value of <0.05 was considered to indicate a significant difference. Differences between group means were analyzed by the Mann-Whitney test. Spearman coefficients and logistic univariate analysis were used to determine association of the different clinical and pathologic parameters with MRSI/DCEMR results. All variables were also included in logistic multivariate models. Classification tables ("2 × 2") were used to calculate sensitivity, specificity, negative predictive value (NPV), positive predictive value (PPV), and accuracy in each feature. Receiver operating characteristic (ROC) curves comparison for each analysis phase was also estimated.

## Results

At baseline, no statistically significant difference in mean age, prostate volume, and PSA levels was found between the two groups of randomization (Table 1). In group B cases were categorized into B1 (both normal MRSI and DCEMR) with 45 of 90 cases (50%), B2 (suspicious MRSI and normal DCEMR) with 6 of 90 cases (6.67%), B3 (normal MRSI and suspicious DCEMR) with 3 of

90 cases (3.33%), and B4 (both suspicious MRSI and DCEMR) with 36 of 90 cases (40%; Table 1).

At the second biopsy, a prostate adenocarcinoma histologic diagnosis was found in 22 of 90 cases (24.4%) in group A and in 44 of 90 cases (48.8%) in group B (*P* = 0.01; Table 1). In particular, in group B a prostate adenocarcinoma was found in 3 of 45 cases (6.67%) with both normal MRSI and DCEMR (B1), in 6 of 6 cases (100%) with suspicious MRSI and normal DCEMR (B2), in 2 of 3 cases (66.6%) with normal MRSI and suspicious DCEMR (B3), and in 33 of 36 cases (91.6%) with both suspicious MRSI and DCEMR (B4; Table 2).

In all cases with a suspicious MRSI and/or DCEMR who were found positive for prostate cancer at the second biopsy, the localization of cancer at histology corresponded to the site indicated by MRSI and/or DCEMR (Table 2).

Sensitivity, specificity, PPV, NPV, and accuracy of MRSI, DCEMR, and their combination are reported in Table 3. ROC curves and area under the curve (AUC) values for MRSI, DCEMR, and the combination of MRSI and DCEMR have been calculated in group B (Fig. 3). AUC was significantly (*P* < 0.001) greater in the combination of MRSI and DCEMR than with MRSI and DCEMR alone.

In group A, 50 cases with a second negative random biopsy accepted to be submitted to MRSI and DCEMR. Of 50 cases, 20 (40%) showed both normal MRSI and DCEMR (A1), 6 (12%) showed suspicious MRSI (A2), 1 (2%) showed suspicious DCEMR (A3), and 23 (46%) showed both suspicious MRSI and DCEMR (A4). At the

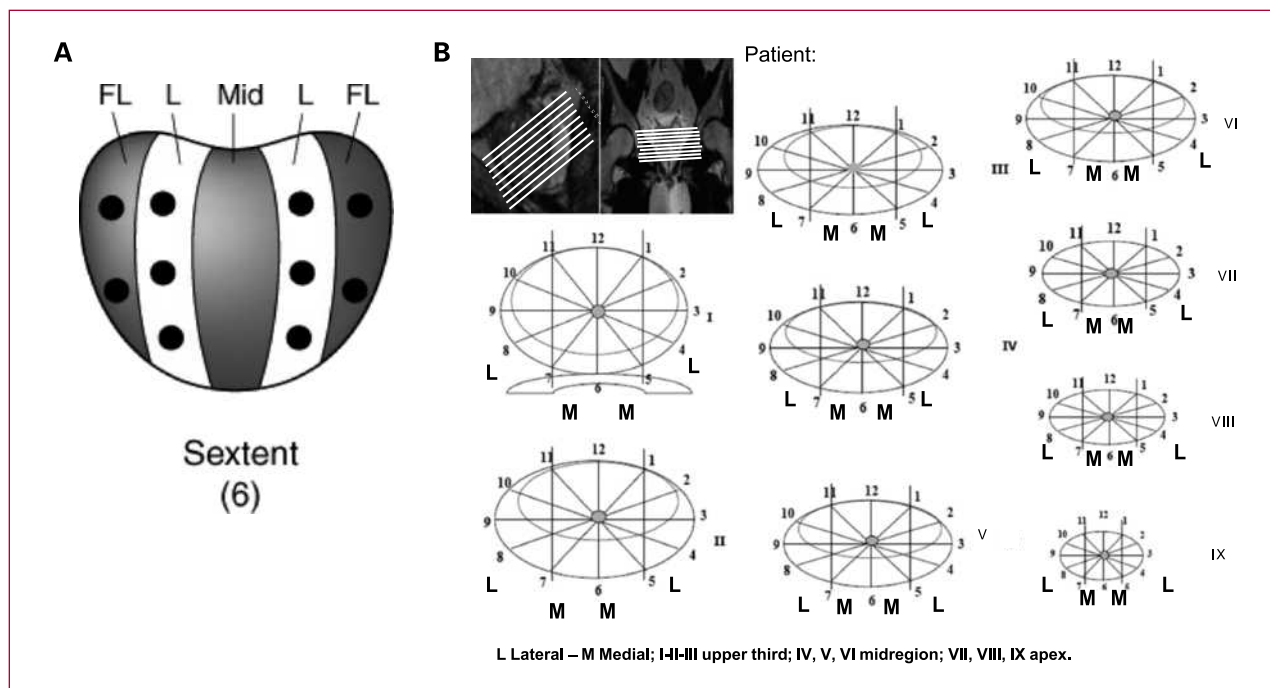


**Fig. 2.** A, 10-core peripheral zone random biopsy sites. Mid, median; L, lateral (traditional sextant biopsies); FL, additional lateral samples. B, site-scheme used at MRSI and DCEMR to localize voxels in the peripheral zone of the prostate.

**Table 2.** Group B. Comparison of MRSI/DCEMR with pathological results at second biopsy

MRI results	Prostate cancer at second biopsy	Correspondence between suspicious MRI voxel and prostate cancer site (at pathology) localization
Both MRSI and DCEMR negative	3/45 cases (6.67%)	No suspicious voxels
Suspicious MRSI and negative DCEMR	6/6 cases (100%)	6/6 cases (100%); 11/12 suspicious voxels (91.6%)
Negative MRSI and suspicious DCEMR	2/3 cases (66.6%)	2/2 cases (100%); 28/35 suspicious voxels (80%)
Both MRSI and DCEMR suspicious	33/36 cases (91.6%)	33/33 cases (100%); 125/132 suspicious voxels (94.6%)

NOTE: Correspondence in the localization between suspicious voxels and prostate cancer site at biopsy.

third biopsy, a prostate adenocarcinoma was found in 1 of 20 cases (5%), 3 of 6 cases (50%), 1 of 1 case (100%), and 21 of 23 cases (91.3%) of A1, A2, A3, and A4, respectively. In all cases with a suspicious MRSI and/or DCEMR who resulted positive for prostate cancer at the third biopsy, the localization of cancer at histology corresponded to the site indicated by MRSI and/or DCEMR. Table 4 shows the sensitivity, specificity, PPV, NPV, and accuracy of MRSI, DCEMR, and their combination in this A subgroup.

On univariate analysis, using group A for comparison, a positive MRSI (suspicious findings), positive DCEMR, and both positive MRSI and DCEMR were all significantly associated ( $r = 0.650$ ; 95% confidence interval, 0.541-0.877; and  $P = 0.0147$ ;  $r = 0.740$ ; 95% confidence interval, 0.600-0.914; and  $P = -0.0011$ ; and  $r = 0.860$ ; 95% confidence interval, 0.701-0.965; and  $P = -0.0001$ , respectively) with the presence of a second positive biopsy, whereas other variables such as age, total PSA, and prostate volume were not significantly associated ( $P > 0.05$ ). At the multivariate analysis only MRSI ( $P = 0.001$ ) and the association of MRSI and DCEMR ( $P = 0.0001$ ) were found to be significant and independent predictors for prostate cancer detection at second biopsy.

## Discussion

The diagnosis of prostate adenocarcinoma is mainly based on the use of PSA determination and TRUS-guided biopsies. MRI of the prostate is not routinely used in the

initial diagnosis of prostate adenocarcinoma, but rather for staging (22).

Urologists often face the dilemma of managing patients with persistently high serum PSA levels and negative biopsy. Simply repeated random biopsies in patients with persistently increasing serum PSA show gradually decreasing results as the number of re-biopsy rounds increases, evolving from a 23% cancer detection rate at the first round to a 17.6%, 11.7%, 8.7%, and 0% at the 2nd, 3rd, 4th, and 5th rounds, respectively (12). Biopsy strategies with an increased number of random biopsy cores have been proposed to reduce false negative (FN) rate (20). However, saturation biopsy can be associated with increased patient morbidity and the issue of whether taking more cores results in the detection of more tumors with low-risk characteristics remain controversial (23). Rabets et al. (24) reported a 29% overall cancer detection rate with a saturation biopsy procedure in a repeat biopsy population. The ideal diagnostic test in the initial work-up of these patients should be able to identify cases in which prostate sites suspicious for cancer are reliably identified to guarantee a higher rate of success by guiding biopsies (20).

The present is the largest randomized prospective study in the literature showing that, in patients with a prior negative prostate biopsy and persistently elevated PSA levels, a combination of a standard 10-core biopsy scheme with an oversampling strategy in sites targeted by combined MRSI/DCEMR indications resulted in significantly higher cancer detection rates. Perrotti et al. (25) and Vilanova et al. (26)

**Table 3.** Group B. Sensitivity, specificity, PPV, NPV, accuracy and AUC of MRSI, DCEMR, and their combination for predicting prostate cancer detection

	Sensitivity	Specificity	PPV	NPV	Accuracy	AUC
Core-by-core analysis						
MRSI	83.3%	72.7%	71.4%	84.2%	77.5%	
DCEMR	75.6%	76.7%	73.6%	78.5%	76.2%	
MRSI+DCEMR	89.7%	80.4%	81.3%	89.1%	85.0%	
Patient-by-patient analysis						
MRSI	92.3%	88.2%	85.7%	93.7%	90.0%	0.73
DCEMR	84.6%	82.3%	78.5%	87.5%	83.3%	0.78
MRSI+DCEMR	92.6%	88.8%	88.7%	92.7%	90.7%	0.87

proposed the idea that prostate adenocarcinoma can be imaged by MRI and, studying the prospective use of MRI to guide biopsy, they showed a slight benefit with a sensitivity of 70% to 83% and a PPV of 12% to 53%. Yuen et al. (10) conducted a study to determine if MRI combined with MRSI can better detect tumor foci in 24 patients with prior negative TRUS biopsy. They concluded that MRI and MRSI have the potential to direct biopsy in these patients with 100% sensitivity, 70.6% specificity, 58.3% PPV, 100% NPV, and 79.2% accuracy for the detection of prostate adenocarcinoma. In their study (10), however, only 57.1% of tumors correlated with MRSI in their localization. Amsellem-Ouazana et al. (11), in a population of 42 cases with negative prostate biopsies and a PSA >4 ng/mL, reported that the sensitivity, specificity, PPV, NPV, and accuracy of MRI/MRSI for the detection of prostate adenocarcinoma was 73.3%, 96.3%, 91.6%, 86.6%, and 88%, respectively. In a population of only 20 cases with similar characteristics, Wetter et al. (22) reported 100% sensitivity and 69% specificity of MRSI for tumor detection. Recently in a population of 54 men with previous negative biopsies and elevated PSA levels, Cirillo et al. (20) reported 100% sensitivity, 51.4% specificity, 48.6% PPV, 100% NPV, and 66.7% accuracy for MRI/MRSI. Lawrentschuk et al. (13) reviewed all available databases for prospective studies in patients using MRI/MRSI and prostate biopsy with previous negative biopsies and persistently elevated PSA levels. Only six studies fulfilled the criteria; all studies had limited populations (the largest was 54 cases; ref. 20), with 215 patients in all. For MRI/MRSI, the overall sensitivity for predicting positive biopsies was 57% to 100%, the specificity 44% to 96%, and the accuracy 67% to 85%.

Our present study is the first randomized prospective study (with the largest population at 180 cases) on this topic. Moreover, for the first time, not only MRSI but also DCEMR and combination MRSI/DCEMR have been investigated in this clinical setting. In our study at the second biopsy, a prostate adenocarcinoma was found in 24.4% of cases in the group submitted to a new random biopsy and in 48.8% of cases in the group in which the second biopsy was also directed on the basis of MRSI/DCEMR results. All the cases (100%) with a suspicious MRSI/DCEMR who were found positive for prostate cancer at histology corresponded to the site indicated by MRSI/DCEMR. In our population, on a patient-by-patient basis, the association of MRSI with DCEMR information did not significantly increase the sensitivity (92.6%), specificity (88.8%), PPV (88.7%), NPV (92.7%), and accuracy (90.7%) for predicting prostate cancer detection when compared with MRSI-alone results. On the contrary, in a subgroup of 50 cases with a negative second random biopsy (group A), MRSI plus DCEMR showed higher values of accuracy (92.0%) when compared with MRSI alone (88.0%).

It is also important to underline that all prostate cancer detected on the basis of MRSI/DCEMR results showed a Gleason score  $\geq 6$  (3+3) and 61.6% a Gleason score  $\geq 7$  (4+3). The positive findings of our study showed in this

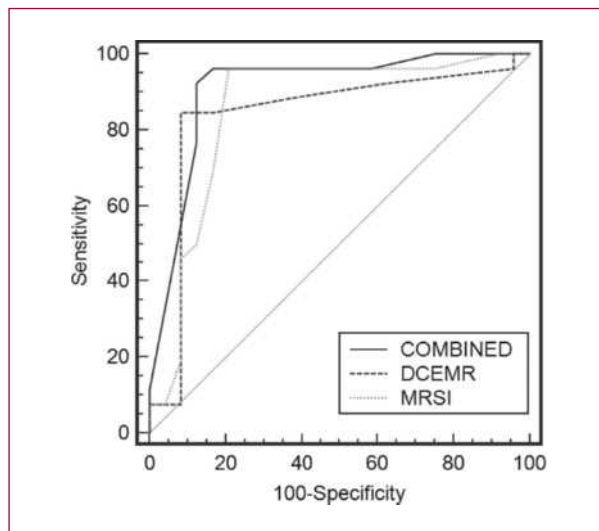


**Fig. 3.** ROC curves comparison for each analysis phase. ROC curves are calculated in group B and show AUC values for MRSI, DCEMR, and the combination of MRSI and DCEMR. AUC was significantly ( $P < 0.001$ ) greater in combination of MRSI and DCEMR than with MRSI and DCEMR alone.

kind of population the potential of these imaging MR techniques for detecting clinically significant cancers in the peripheral zone of the prostate. Therefore, MRI targeted biopsies may delineate significant cancers more often than standard random schemes. Similarly Zakian et al. (27) confirmed that high-grade tumors are more likely to be detected on MRSI.

The significance of the results obtained in the present study may be due to the criteria used to design the study and to evaluate MRSI/DCEMR results. First, this was a prospective randomized study on a large homogeneous population. Second, all random biopsies were homogeneously carried out by the same physician (MC) and all following a 10-core laterally directed TRUS-guided scheme as in previous experiences (14). Third, strict criteria were used when defining abnormal areas at MR. We decided not to introduce an intermediate class for inconclusive or equivocal findings (20). In particular for MRSI we defined the choline + creatine/citrate ratio threshold for cancer suspicious at 0.80, as previously reported in the literature by some experience (10, 11, 20). The positive findings of our study showed the potential of these qualitative criteria. On the contrary, Wetter et al. (22) in their analysis, on the basis of the choline + creatine/citrate ratio, defined three categories: normal if below 0.6; borderline from 0.6 to 1.1, and pathologic for above 1.1. Amsellem et al. (11) reported a significant reduction in the specificity and PPV of MRSI when reducing the threshold of the ratio from 0.8 to 0.75, due to the increase of MRSI FP findings.

However, there are also limitations to this study. We limited our analysis to the peripheral zone of the prostate as it is well known that MR and MRSI evaluation are both inadequate in the differential diagnosis between adenoma and cancer arising from the transition region of

**Table 4.** A subgroup of 50 cases with negative second random biopsy

	Sensitivity	Specificity	PPV	NPV	Accuracy
MRSI	92.3%	79.1%	83.3%	95.0%	88.0%
DCEMR	84.6%	91.6%	91.6%	84.6%	88.0%
MRSI+DCEMR	93.1%	90.4%	93.1%	90.4%	92.0%

NOTE: Sensitivity, specificity, PPV, NPV, and accuracy of MRSI, DCEMR, and their combination for predicting prostate cancer detection.

the prostate (13, 20). As has been previously reported, matching abnormal MR regions to TRUS to guide biopsies can present limitations (20). Difficulties in ensuring the correspondence of TRUS biopsy spatial accuracies to suspicious areas on MRSI/DCEMR have been reported by several studies with a similar design (10). In our analysis, however, for comparison of MR with pathologic data, the peripheral zone of the prostate was divided in sextants according to strict criteria (17, 18). Assessment of the spatial correspondence between MRSI and DCEMR findings and the pathological evaluation was done by a single investigator who was not a reader of MR images. The 100% correspondence between the localization of cancer at histology and the site indicated by MRSI/DCEMR in cases with suspicious MRSI/DCEMR who were found positive for prostate cancer at biopsy supported our methodology. However, it is true that the spatial association of directed TRUS biopsy can be better assessed submitting cases to radical prostatectomy and correlating MR findings with step section histopathology (10). Another limitation of our study is that in group B patients had more samples than patients in group A, on the basis of MRI/DCEMR results. However, we believe that some data supported that the better results obtained in group B than in group A are more related to MRI methodology than to an increased number of biopsy samples. First and most important, the 100% correspondence between the localization of cancer at histology and the site indicated by MRSI/DCEMR in cases with suspicious MRSI/DCEMR who were found positive for prostate cancer at biopsy supported our methodology. Second, the role of saturation random biopsy is currently controversial and still debated. Many experiences with saturation random biopsy taking  $\geq 24$  cores in a similar population reported a detection rate between 30% and 42%, emphasizing the risk of diagnosing clinically insignificant prostate cancer and the need to target prostate cancer with novel imaging techniques (23, 24). Assuming that the problem is not overdiagnosis but a potential over-treatment, in our experience taking a median of 12.17

cores in group B, we report a detection rate of 48.8% and an high rate of clinically significant prostate cancer [61.6% with Gleason score  $\geq 7$  (4+3)]. Third, for avoiding a potential bias related to the number of samples, in group A, 50 cases with a second negative random biopsy accepted to be submitted to MRSI plus DCEMR, and at the third biopsy, a prostate adenocarcinoma was found in 21 of 23 cases (91.3%) with both suspicious MRSI and DCEMR but only in 1 of 20 cases (5%) with both normal MRSI/DCEMR, and in all cases with a suspicious MRSI and/or DCEMR who were found positive for prostate cancer at the third biopsy, the localization of cancer at histology corresponded to the site indicated by MRSI and/or DCEMR. For all these reasons, we believe that the better results obtained in group B than in group A can be explained by the role of MRI methodology rather than an increased number of biopsy samples.

In conclusion, the combination of MRSI and DCEMR in our population showed the potential to guide biopsy to cancer foci in patients with previously negative TRUS biopsy. This should represent a reasonable approach in a group of patients who often have tremendous psychological stresses due to the uncertain diagnosis obtained with random repeated biopsies in the face of persistently abnormal PSA (10). In the future a MRSI/DCEMR directed biopsy could be prospectively compared with a saturation biopsy procedure to assess not only their respective accuracy but also morbidity and cost-effectiveness.

#### Disclosure of Potential Conflicts of Interest

No potential conflicts of interest were disclosed.

#### Acknowledgments

The costs of publication of this article were defrayed in part by the payment of page charges. This article must therefore be hereby marked *advertisement* in accordance with 18 U.S.C. Section 1734 solely to indicate this fact.

Received 08/13/2009; revised 01/19/2010; accepted 01/20/2010; published OnlineFirst 03/02/2010.

#### References

- Seitz M, Shukla-Dave A, Bjartell A, et al. Functional magnetic resonance imaging in prostate cancer. *Eur Urol* 2009, [Epub ahead of print]55:801–14.
- Panebianco V, Sciarra A, Osmani M, et al. 2D and 3D T2-weighted MR sequence for the assessment of neurovascular bundles changes after nerve sparing radical prostatectomy with erectile function correlation. *Eur Radiol* 2009;19:220–9.
- Kirkham AP, Emberton M, Allen C. How good is MRI at detecting

- and characterising cancer within the prostate? *Eur Urol* 2006;50:1163–75.
4. Anastasiadis AG, Lichy MP, Nagele U, et al. MRI-guided biopsy of the prostate increases diagnostic performance in men with elevated or increasing PSA levels after previous negative TRUS biopsies. *Eur Urol* 2006;50:738–49.
  5. Rajesh A, Coakley FV, Khrhanewicz J. 3D spectroscopic imaging in the evaluation of prostate cancer. *Clin Radiol* 2007;62:921–9.
  6. Hricak H. MR imaging and MR spectroscopic imaging in the pre-treatment evaluation of prostate cancer. *Br J Radiol* 2005;78:103–11.
  7. Rajesh A, Coakley FV. MR imaging and MR spectroscopic imaging of prostate cancer. *Magn Reson Imaging Clin N Am* 2004;12:557–79.
  8. Casciani E, Gualdi G. Prostate cancer: value of magnetic resonance spectroscopy 3D chemical shift imaging. *Abdom Imaging* 2006;31:490–9.
  9. Sciarra A, Salciccia S, Panebianco V. Proton spectroscopic and dynamic contrast-enhanced magnetic resonance: a modern approach in prostate cancer imaging. *Eur Urol* 2008;54:485–8.
  10. Yuen JSP, Thng CH, Tan PH, et al. Endorectal magnetic resonance imaging and spectroscopy for the detection of tumor foci in men with prior negative transrectal ultrasound prostate biopsy. *J Urol* 2004;171:1482–6.
  11. Amsellem-Ouazana D, Younes P, Conquy S, et al. Negative prostatic biopsies in patients with high risk of prostate cancer. Is the combination of endorectal MRI and magnetic resonance spectroscopy imaging (MRSI) a useful tool? A preliminary study. *Eur Urol* 2005;47:582–6.
  12. Zackrisson B, Aus G, Bergdahl S. The risk of findings focal cancer (less than 3 mm) remains high on re-biopsy of patients with persistently increased prostate specific antigen but the clinical significance is questionable. *J Urol* 2004;171:1500–3.
  13. Lawrentschuk N, Fleshner N. The role of magnetic resonance imaging in targeting prostate cancer in patients with previous negative biopsies and elevated prostate-specific antigen levels. *BJU Int* 2009;103:730–3.
  14. Sciarra A, Autran Gomez A, Salciccia S, et al. Biopsy-derived Gleason artifact and prostate volume: experience using ten samples in larger prostates. *Urol Int* 2008;80:145–50.
  15. Kumar R, Nayyar R, Kumar V. Potential of magnetic resonance spectroscopic imaging in predicting absence of prostate cancer in men with serum prostate-specific antigen between 4 and 10 ng/mL: a follow-up study. *Urology* 2008;72:859–63.
  16. Sciarra A, Panebianco V, Salciccia S. Role of dynamic contrast-enhanced magnetic resonance (MR) imaging and proton MR spectroscopic imaging in the detection of local recurrence after radical prostatectomy for prostate cancer. *Eur Urol* 2008;54:589–600.
  17. Wefer AE, Hricak H, Vigneron DB, et al. Sextant localization of prostate cancer: comparison of sextant biopsy, magnetic resonance imaging and magnetic resonance spectroscopic imaging with step section histology. *J Urol* 2000;164:400–4.
  18. Testa C, Schiavina R, Lodi R, et al. Prostate cancer: sextant localization with MR imaging, MR spectroscopy, and 11c-choline PET/CT. *Radiology* 2007;244:797–806.
  19. Kurhanewicz J, Vigneron DB, Hricak H, et al. Prostate cancer: metabolic response to cryosurgery as detected with 3D H-1 MR spectroscopic imaging. *Radiology* 1996;200:489–96.
  20. Cirillo S, Petracchini M, Della Monica P, et al. Value of endorectal MRI and MRS in patients with elevated prostate-specific antigen levels and previous negative biopsies to localize peripheral zone tumors. *Clinical Radiology* 2008;63:871–9.
  21. Fütterer JJ, Heijmink SW, Scheenen TW, et al. Prostate cancer localization with dynamic contrast-enhanced MR imaging and proton MR spectroscopic imaging. *Radiology* 2006;241:449–58.
  22. Wetter A, Hübner F, Lehnert T, et al. Three-dimensional 1H-magnetic resonance spectroscopy of the prostate in clinical practice: technique and results in patients with elevated prostate-specific antigen and negative or no previous prostate biopsies. *Eur Radiol* 2005;15:645–52.
  23. Scattoni V, Zlotta A, Montironi R, Schulman C, Rigatti P, Montorsi F. Extended and saturation prostatic biopsy in the diagnosis and characterisation of prostate cancer: a critical analysis of the literature. *Eur Urol* 2007;52:1309–22.
  24. Rabets JC, Jones JS, Patel A, Zippe CD. Prostate cancer detection with office based saturation biopsy in a repeat biopsy population. *J Urol* 2004;172:94–7.
  25. Perrotti M, Han KR, Epstein RE, et al. Prospective evaluation of endorectal magnetic resonance imaging to detect tumor foci in men with prior negative prostatic biopsy: a pilot study. *J Urol* 1999;162:1314–22.
  26. Vilanova JC, Comet J, Capdevila A, et al. The value of endorectal MR imaging to predict positive biopsies in clinically intermediate-risk prostate cancer patients. *Eur Radiol* 2001;11:29–35.
  27. Zakian KI, Sircar K, Hricak H, et al. Correlation of proton MR spectroscopic imaging with gleason score based on step-section pathologic analysis after radical prostatectomy. *Radiology* 2005;234:804–14.
  28. Delongchamps NB, Hass GP. Saturation biopsies for prostate cancer: current uses and future prospects. *Nat Rev Urol* 2009;6:645–52.